Available online at www.sciencedirect.com
ScienceDirect
Journal of Sound and Vibration 299 (2007) 900–917
JOURNAL OF SOUND AND VIBRATION
www.elsevier.com/locate/jsvi

Forced vibro-acoustical analysis for a theoretical model of a passenger compartment with a trunk—Part I: Theoretical part

Jin Woo Lee[a,*], Jang Moo Lee[b]

[a]*R&D Center, Digital Appliance Business, Samsung Electronics Co. Ltd., 416 Maetan-3-dong, Yeongtong-Gu, Suwon-City, Gyeonggi-Do 443-742, Republic of Korea*
[b]*School of Mechanical and Aerospace Engineering, Seoul National University, San 56-1, Shillim-dong, Kwanak-gu, Seoul 151-742, Republic of Korea*

Received 6 December 2005; received in revised form 2 May 2006; accepted 24 July 2006
Available online 20 October 2006

Abstract

In this paper, a new analytical model is proposed to investigate interior noise in a passenger compartment of an automobile with a trunk. The new analytical model is a coupled structural–acoustic model, which consists of double cavities connected by a neck and two mechanical harmonic oscillators. Acoustic impedance is calculated at every surface of discontinuity in the cross-sectional area for the forced vibro-acoustical analysis of the coupled system. Evanescent wave as well as standing wave is considered to investigate the neck's effect on modal properties of the coupled system. The evanescent wave with a set of cross-modes is converted to an added length term of the neck. In deriving the characteristic equation of the coupled system, the real length of a neck is replaced by the effective length including the added length. A new coupling parameter, which changes the natural frequencies of the coupled system, is introduced and is compared with other coupling parameters (mass ratio and stiffness ratio) in case studies. The natural frequencies of the coupled system decrease as the value of the new coupling parameter increases, which means that the cross-sectional area of the neck decreases and its position shifts close to the corner. Also, the results in this paper are qualitatively validated by an experimental investigation in a companion paper, Part 2.

1. Introduction

In many engineering situations, noise and vibration problems generated by structural–acoustic coupling can be encountered. Coupling between an acoustic cavity and a surrounding elastic body strongly affects the interior noise of a vehicle compartment in the low-frequency range [1]. Fluid loading has been considered an important factor in the vibration of an elastic plate of vibrating machinery in contact with heavy fluid such as water [2]. The general acoustic characteristics of a coupled structural–acoustic system consisting of a simple rectangular or circular cavity and a simply supported or clamped plate have been theoretically and

*Corresponding author. Present address: National Creative Research Initiatives Center for Multiscale Design (311-206), School of Mechanical and Aerospace Engineering, Seoul National University, Seoul, 151-742, Republic of Korea. Tel.: +82 31 218 5205; fax: +82 31 218 5196.
E-mail address: jw062nam@yahoo.co.kr (J.W. Lee).

0022-460X/$ - see front matter © 2006 Elsevier Ltd. All rights reserved.
doi:10.1016/j.jsv.2006.07.022

Nomenclature

c	sound velocity
$\tilde{f}_1(t)$	external harmonic force
f_i^a	natural frequency of a rigid-wall cavity
f_i^c	natural frequency of the coupled system
f^s	natural frequency of an oscillator
$2h_i$	height of a cavity ($i = 1, 2$) or a neck ($i = n$)
H_{i1}	height ratio between cavity $2(i = 2)$ or a neck ($i = n$) and cavity 1
j	imaginary unit, $\sqrt{-1}$
k	wave number ($= \omega/c$)
${}_ik_q$	wave number in the y-direction of the ith cavity
${}_ik_s$	wave number in the z-direction of the ith cavity
l_i	length of a cavity ($i = 1, 2$) or a neck ($i = n$)
l'_n	effective length of a neck
L_{i1}	length ratio between cavity $2(i = 2)$ or a neck ($i = n$) and cavity 1
L'_{n1}	non-dimensional effective length
ΔL_{n1}	non-dimensional added length
Δl_i	added length of the ith cavity
Δl_n	total added length of a neck ($= \Delta l_1 + \Delta l_2$)
m_i	mass of a mechanical oscillator
m_i^a	equivalent mass of the acoustic medium in the ith cavity
u	time independent velocity fluctuation
$\tilde{p}_i$	acoustic pressure of a cavity ($i = 1, 2$) or a neck ($i = n$)
R_i	damping coefficient
s_i	spring constant of a mechanical oscillator
s_i^a	equivalent stiffness of the acoustic medium in the ith cavity
S	cross-sectional area of a surface
S_i	cross-sectional area of a cavity ($i = 1, 2$) or a neck ($i = n$)
S_{i1}	cross-sectional area ratio between cavity $2(i = 2)$ or a neck ($i = n$) and cavity 1
t	time
$2w_i$	width of a cavity ($i = 1, 2$) or a neck ($i = n$)
W_{i1}	width ratio between cavity $2(i = 2)$ or a neck ($i = n$) and cavity 1
Z	acoustic impedance
Z_i	acoustic impedance at point i.
$Z_i^{(m)}$	mechanical impedance at point i.
Z_{c_i}	acoustic impedance in cavity $i(i = 1, 2)$.
$\bar{Z}_i$	non-dimensional acoustic impedance at point i.
$\bar{Z}_i^{(m)}$	non-dimensional mechanical impedance at point i.

Greek symbols

${}_i\alpha_{x_{qs}}$	$\sqrt{{}_ik_q^2 + {}_ik_s^2 - k^2}$
ρ_a	density of acoustic medium
Ω	non-dimensional frequency ($= kl_1/\pi$)
Ω^s	non-dimensional natural frequency of an oscillator
Ω_i^a	non-dimensional natural frequencies of a cavity
Ω_i^c	non-dimensional natural frequencies of a coupled system
$\tilde{\xi}_n$	displacement of a lumped mass element in a neck
$\tilde{\xi}_i$	displacement of the ith oscillator
ω	angular frequency

Superscripts

a	acoustic medium or cavity
c	a coupled system
s or (m)	a mechanical oscillator
$+,-$	right and left of a specific point

Subscripts

i	number of a cavity or a mechanical oscillator
n	a neck

experimentally discussed in terms of natural frequencies and natural modes in the previous researches [3–8]. And, to investigate the coupling effect of a coupled system with special acoustic characteristics, a particular theoretical model has been introduced [9,10].

Our works suggest a new theoretical model, which can best represent interior noise in the passenger compartment of an automobile with a trunk in the low-frequency range. A package tray in the real car has

several holes for speakers and electric devices, and air ventilation holes for air leakage when side doors are closed. Since a passenger compartment cavity is acoustically connected to the trunk compartment cavity through the package tray, the longitudinal acoustic modes, which strongly contribute to the booming noise of the vehicle, are affected by the trunk cavity and by a trunk lid [11]. Therefore, case studies on the new coupled system can provide better understanding of the acoustic characteristics of a passenger car with a trunk and information on the reduction of the booming noise. And, simulation results show that acoustical modification can change the coupling degree of the coupled system.

Many theoretical models have been introduced to exactly explain and predict the dynamic behavior of coupled structural–acoustic systems, which have been too complicated to directly analyze. Although these models were simplified systems, they were very informative in helping us understand the acoustic characteristics of a real coupled system. Results obtained from theoretical investigations such as parametric studies have been useful in partially modifying a real system to have desirable acoustic characteristics. For example, to reduce interior noise in cars, spacecraft and airplanes, one-dimensional coupled structural–acoustic system was suggested, and the effect of geometrical and physical parameters on the natural frequencies of the coupled system was investigated [12–14].

Some researchers investigated a one-dimensional rectangular or circular cavity coupled to a simple structural system. Cura et al. [12] considered a uni-dimensional acoustic cavity coupled to a one-degree-of-freedom system as an analytical model to experimentally and analytically study the vibro-acoustical behavior of the system excited by a harmonic force. And Scarpa and Curti [13] used a rectangular acoustic cavity closed at one end by a simply supported plate to present an algorithm that can compute the sensitivities of the frequencies versus design parameters (plate thickness and cavity width). Hong and Kim [14] formulated the governing equations of a one-dimensional acoustic pipe whose one end was closed and the other end was attached to a one-degree-of-freedom mass–spring system (a mechanical harmonic oscillator). Also, they developed a solution procedure for a one-dimensional system to analyze a coupled structural–acoustic system with viscous or structural damping and absorbing material [15]. Lyon [16] used a small rigid enclosure backed by one flexible wall to study the theoretical noise reduction according to frequency range. Magalhaes [17] developed a one-dimensional component mode synthesis (CMS) model to analyze and calculate sound transmission through a limp mass panel between connected acoustic volumes. Dowell [18] investigated the effect of a cavity on panel using a rectangular cavity of which one side was a vibrating plate, and illustrated the change in the natural frequencies in terms of aerodynamics.

Other researchers have suggested advanced analytical methods for new theoretical models and applied the results to finite element models for predicting and modifying interior noise in a coupled structural–acoustic system. Sung [19] suggested an analytical method to identify noise sources and to predict interior noise of an automotive vehicle by using finite element models. Nefske [20] investigated the acoustics of an automobile passenger compartment by using the brief formulation of the finite element method for structural–acoustical analysis. Han [21] developed a hybrid model to predict the vibro-acoustic response of structures excited by complex turbulent flow. Trompette [22] predicted the vibro-acoustic behavior of the metal box by using FE model and BE model, which were adjusted by comparing the natural frequencies calculated from the models with those measured through experiments. Campbell [23] defined body acoustic sensitivity to use as a noise transfer function for structural–acoustic coupling analysis and showed that an analytical method for predicting body acoustic sensitivity could be used early in the design process using finite element model.

We propose a new coupled structural–acoustic model composed of double cavities connected by a neck and mechanical harmonic oscillators to identify the acoustic characteristics of a passenger compartment with a trunk compartment, and a plane wave theory is applied to the new coupled model. Acoustic impedances at every surface of discontinuity in the cross-sectional area are calculated for forced vibro-acoustical analysis of the suggested theoretical model: the acoustic response of the system to an external force is calculated. All parameters and coefficients are written in dimensionless forms for the case studies. Three coupling parameters are developed from the process of deriving the characteristic equation. The first parameter is mass ratio between the air in the cavity and the mechanical oscillator that backs the cavity, the second one is the ratio between the equivalent stiffness of air in the cavity and the stiffness of the mechanical oscillator, and the third is a new coupling parameter, which is defined as the non-dimensional effective length of the neck divided by the cross-sectional area ratio between the neck and the cavity. While the first two coupling parameters have

been considered in the many previous papers, the new coupling parameter, which can explain the effect of the cross-sectional area and position of the neck on coupling degree, has hardly ever been dealt with as a coupling parameter of a coupled system. We will examine the influence of the last coupling parameter on our coupled system and compare it with that of the first two parameters for four cases depending on the natural frequency of the mechanical harmonic oscillator. Experiments supporting the results of the theoretical model in this paper will be conducted in the companion paper, Part 2.

2. Theoretical model for forced vibro-acoustical analysis

Fig. 1 shows a theoretical model investigated in the forced vibro-acoustical analysis: two rectangular cavities of the same cross-section are connected by a neck and blocked by two mechanical harmonic oscillators (mass–spring–damper system) at both ends. This simplified model represents a passenger compartment acoustically connected to a trunk compartment. The neck has a cross-sectional area of $S_n(= 2w_n \times 2h_n)$, and its length l_n is so small compared to the cavity length that the neck can be regarded as a lumped mass. S_i denotes the cross-sectional area of each cavity, whose lengths, widths and heights are denoted by l_i, $2w_i$ and $2h_i$, respectively. Cavity 1 is blocked by an oscillator at $x = b$ and cavity 2 blocked by the same oscillator at $x = 0$. S_i, m_i and R_i designate the spring constant, mass and damping coefficients, respectively. External harmonic force $\tilde{f}_1(t)$ applied at $x = b$ generates the displacements $\tilde{\xi}_1(t)$ and $\tilde{\xi}_2(t)$ of the two mechanical oscillators and the acoustic pressures $\tilde{p}_1(x, t)$ and $\tilde{p}_2(x, t)$ in the two cavities.

2.1. Plane wave theory and evanescent wave

In general, the concept of acoustic impedance is useful for acoustical analysis of a pipe or a long cavity, whose acoustical properties in the low-frequency range change along only one direction but not along the other directions [24]. And it is convenient to represent the frequency response characteristics in terms of acoustic impedance in investigating the forced response of an acoustic medium derived by a mechanical oscillator [25–27]. The use of acoustic impedance Z is based on the plane wave, whose acoustical variables have constant amplitude on a given plane perpendicular to the direction of wave propagation [28], and is defined as acoustic pressure p divided by volume velocity at the surface:

$$Z = p/(S \cdot u), \tag{1}$$

where S is cross-sectional area and u is velocity.

Assuming that the lengths of two cavities, which are connected by a neck, are much longer than their widths and heights, the acoustic field of each cavity in the low frequency range consists of a standing wave and an evanescent wave in the x-direction. The standing wave is superposed by a forward-traveling wave and a

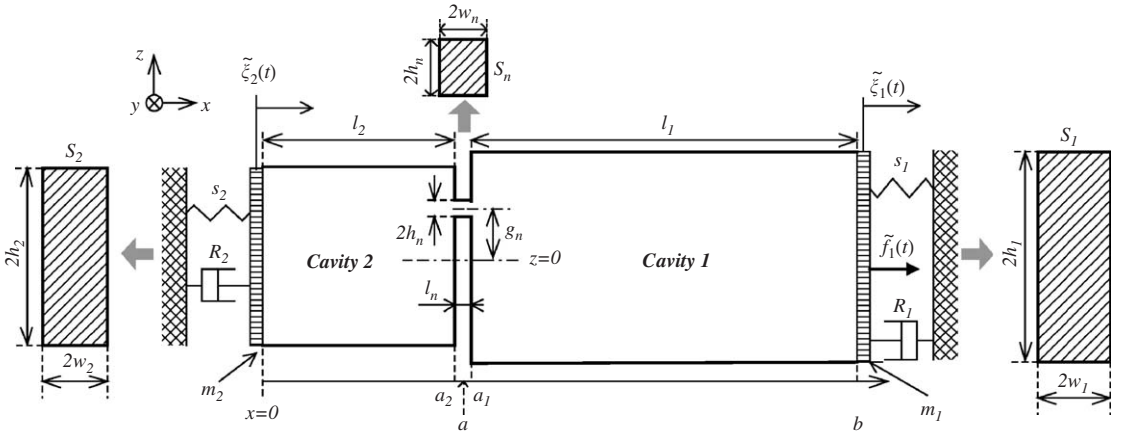

Fig. 1. The coupled system composed of double cavities connected by a neck and two mechanical harmonic oscillators.

backward-traveling wave in the x-direction, and the evanescent wave, which is created due to the cross-sectional discontinuity at the interface between neck and cavity, decays away from the neck. Therefore, acoustical properties around the interface do not have constant amplitude on the perpendicular plane because the evanescent wave is a decaying wave with a set of cross-modes. It seems that acoustic impedance cannot be used for this forced vibro-acoustical analysis. But, since evanescent waves can be converted to the added length of a neck [29], acoustic impedance can be used for this simplified theoretical model if an effective length including the added length replaces the real length of a neck.

2.2. Input acoustic impedance

Input acoustic impedance Z_{b^+} on the right-hand side of the driver in the coupled system shown in Fig. 1 can be expressed by the series combination of mechanical impedance of the driver $Z_b^{(m)}$ and acoustic impedance Z_{b^-} on the left-hand side of the driver:

$$Z_{b^+} = Z_b^{(m)}/S_1^2 - Z_{b^-}, \tag{2}$$

where the mechanical impedance of the driver is

$$Z_b^{(m)} = R_1 + \mathrm{j}(m_1 \cdot \omega - s_1/\omega). \tag{3}$$

Acoustic impedance Z_{b^-} on the left-hand surface at $x = b$ is expressed as a function of acoustic impedance $Z_{a_1^+}$ on the right-hand side at $x = a_1$:

$$Z_{b^-} = Z_{c_1}\frac{Z_{a_1^+} - \mathrm{j}Z_{c_1}\tan(kl_1)}{Z_{c_1} - \mathrm{j}Z_{a_1^+}\tan(kl_1)}, \tag{4}$$

where $Z_{c_1} = \rho_a c/S_1$, ρ_a being the density of the acoustic medium, is the acoustic impedance in cavity 1. And the acoustic impedance $Z_{a_1^+}$ is represented by the series combination of $Z_{a_2^-}$ on the left-hand side at $x = a_2$ and the neck's mechanical impedance $Z_n^{(m)}$:

$$Z_{a_1^+} = Z_{a_2^-} - Z_n^{(m)}/S_n^2, \tag{5}$$

$$Z_n^{(m)} = \mathrm{j}\omega\rho_a l'_n S_n, \tag{6}$$

where the effective length of the neck l'_n consists of the real length of the neck and the added length: $l'_n = l_n + \Delta l_1 + \Delta l_2$. Evanescent wave, which is generated around the neck due to the discontinuity in the cross-sectional area at the interface between the neck and the cavity, is converted to the added length term. And the added length of the ith cavity is represented in terms of geometric parameters [29].

$$\Delta l_i = \frac{S_i}{S_n}\sum_{q=0}\sum_{s=0}\frac{1}{{}_i\alpha_{qs}}\,{}_i\varepsilon_{qsi}\phi_{qi}^2\phi_s^2,\ {}_i\varepsilon_{qs} = \begin{cases} 1, & q\neq 0 \text{ and } s\neq 0, \\ 2, & \text{otherwise}, \end{cases} \tag{7}$$

$${}_i\phi_q = \int_{-w_n}^{w_n}\cos({}_ik_q(y-w_i))\,\mathrm{d}y \Big/ \int_{-w_i}^{w_i}\cos^2({}_ik_q(y-w_i))\,\mathrm{d}y, \tag{8}$$

$${}_i\phi_s = \int_{-h_n}^{h_n}\cos({}_ik_s(z-h_i))\,\mathrm{d}z \Big/ \int_{-h_i}^{h_i}\cos^2({}_ik_s(z-h_i))\,\mathrm{d}z, \tag{9}$$

$${}_i\alpha_{x_{qs}} = -\mathrm{j}k_x = \sqrt{{}_ik_q^2 + {}_ik_s^2 - k^2}, \tag{10}$$

where $k = \omega/c$, ${}_ik_q = q\pi/(2w_i)$ and ${}_ik_s = s\pi/(2h_i)$.

Using Z_{0^+}, acoustic impedance $Z_{a_2^-}$ on the left-hand side at $x = a_2$ becomes

$$Z_{a_2^-} = Z_{c_2} \frac{Z_{0^+} - \mathrm{j}Z_{c_2} \tan(kl_2)}{Z_{c_2} - \mathrm{j}Z_{0^+} \tan(kl_2)}, \tag{11}$$

where $Z_{c_2} = \rho_a \cdot c/S_2$ is the acoustic impedance in cavity 2.

Also, Z_{0^+} is represented by the series combination of the acoustic impedance Z_{0^-} on the left-hand side at $x = 0$ and the mechanical impedance $Z_0^{(m)}$of the oscillator:

$$Z_{0^+} = Z_{0^-} - Z_0^{(m)}/S_2^2, \tag{12}$$

$$Z_0^{(m)} = R_2 + \mathrm{j}(m_2\omega - s_2/\omega). \tag{13}$$

The characteristic equation of the coupled system can be obtained when the reactance of the input impedance is equal to zero as expressed by Eq. (14) [28]:

$$\mathrm{Im}[Z_{b^+}] = 0. \tag{14}$$

Dividing both sides of each equation by Z_{c_1}, variables involved in Eqs. (2)–(14) are rewritten in dimensionless forms for case studies.

$$\bar{Z}_{b^+} = Z_{b^+}/Z_{c_1} = \bar{Z}_b^{(m)} - \bar{Z}_{b^-}, \tag{15}$$

$$\bar{Z}_b^{(m)} = \frac{Z_b^{(m)}}{S_1^2 Z_{c_1}} = \frac{R_1}{\rho c S_1} + \mathrm{j}\left(\frac{m_1}{m_1^a}\Omega\pi - \frac{s_1}{s_1^a}\frac{1}{\Omega\pi}\right), \tag{16}$$

where $\Omega = f/(c/(2l_1))$ denotes the non-dimensional excitation frequency, and $m_1^a = \rho_a l_1 S_1$ and $s_1^a = \rho_a c^2 S_1^2/V_1$ are the equivalent mass and the equivalent stiffness of the acoustic medium in cavity 1, respectively.

$$\bar{Z}_{b^-} = \frac{Z_{b^-}}{Z_{c_1}} = \frac{\bar{Z}_{a_1^+} - \mathrm{j}\tan(\Omega\pi)}{1 - \mathrm{j}\bar{Z}_{a_1^+}\tan(\Omega\pi)}, \tag{17}$$

$$\bar{Z}_{a_1^+} = \bar{Z}_{a_2^-} - \bar{Z}_n^{(m)}, \tag{18}$$

$$\bar{Z}_n^{(m)} = \frac{Z_n^{(m)}}{S_n^2 Z_{c_1}} = \mathrm{j}\Omega\pi\frac{L'_{n1}}{S_{n1}}, \tag{19}$$

where $L'_{n1} = l'_n/l_1$ is the non-dimensional effective length of the neck and S_{n1} the cross-sectional area ratio between the neck and cavity 1.

$$\bar{Z}_{a_2^-} = \frac{1}{S_{21}}\frac{\bar{Z}_{0^+}S_{21} - \mathrm{j}\tan(\Omega\pi L_{21})}{1 - \mathrm{j}\bar{Z}_{0^+}S_{21}\tan(\Omega\pi L_{21})}, \tag{20}$$

$$\bar{Z}_{0^+} = \bar{Z}_{0^-} - \bar{Z}_0^{(m)}, \tag{21}$$

$$\bar{Z}_0^{(m)} = \frac{Z_0^{(m)}}{S_2^2 Z_{c_1}} = \frac{1}{S_{21}}\left(\frac{R_2}{\rho c S_2} + \mathrm{j}\left(\frac{m_2}{m_2^a}\Omega\pi L_{21} - \frac{s_1}{s_2^a}\frac{1}{\Omega\pi}\frac{1}{L_{21}}\right)\right), \tag{22}$$

where $m_2^a = \rho_a l_2 S_2$ and $s_2^a = \rho_a c^2 S_2^2/V_2$ are the equivalent mass and the equivalent stiffness of the acoustic medium in cavity 2, respectively. S_{21} and L_{21} are the cross-sectional area ratio and the length ratio between cavity 2 and cavity 1, respectively.

3. Case studies

Equations developed in the previous section are applied to two analytical models. The first analytical model (See Fig. 2) represents double cavities connected by a neck and blocked by an oscillator at one end ($x = b$) and corresponds to the passenger compartment cavity with a trunk cavity excluding the trunk lid. The second

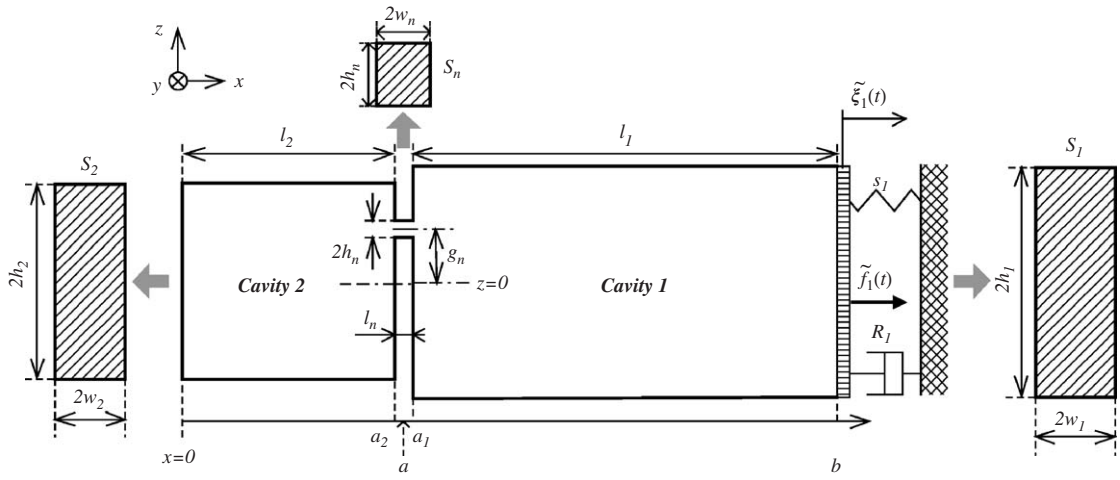

Fig. 2. Double rectangular cavities connected by a neck and blocked by a mechanical oscillator at one end.

model (See Fig. 1), which consists of double cavities connected by a neck and two oscillators at both ends, represents the passenger compartment cavity with a trunk cavity including a trunk lid. Also, two kinds of natural frequency of the oscillators are used in each case study because the proximity in the natural frequency f^s of an oscillator and the natural frequency f_i^a of the rigid-wall cavity mode affects the ith coupled natural frequencies f_i^c of the coupled system; $f^s < f_1^a$ (the 1st oscillator); and $f^s = f_1^a$ (the 2nd oscillator). Analytical results explain the effect of four factors on the modal properties of the coupled systems: mass ratio; stiffness ratio; a neck's cross-sectional area; and a neck's position.

For the convenience of analysis, cavity 1 and cavity 2 have the same rectangular cross-section ($2w_1 = 2w_2 = 0.64\,\text{m}$, $2h_1 = 2h_2 = 0.44\,\text{m}$ and $W_{21} = 1, H_{21} = 1$) and the width of the neck is the same as widths of cavity 1 and cavity 2 ($W_{n1} = 1$). But, neck's length is twelve-thousandths of that of cavity 1 ($L_{n1} = 0.012$) and its height is one-tenth of height of cavity 1 ($H_{n1} = 0.1$). Length ratio between cavity 2 and cavity 1 is 0.34 ($L_{21} = 0.34$). Also, acoustic medium is air: density ρ_a is $1.12\,\text{kg/m}^3$; and sound velocity c is 340 m/s.

Mass 2.20 kg of the first oscillator is calculated from a real steel plate of $440 \times 640 \times 1\,\text{mm}$, and its natural frequency, which is determined from a clamped real steel plate by Galerkin's Method, is less than the first natural frequency of the double cavities: $f^s < f_1^a$. Stiffness ($1.09 \times 10^5\,\text{N/m}$) is calculated by the mass and the natural frequency determined previously. Therefore, the non-dimensional natural frequency Ω^s of the first oscillator, mass ratio m_1/m_1^a and stiffness ratio s_1/s_1^a are 0.21, 6.45 and 2.77, respectively.

And, with its mass fixed at 2.20 kg, the stiffness of the second oscillator is adjusted so that f^s coincides with f_1^a. Therefore, non-dimensional natural frequency Ω^s of the oscillator, mass ratio m_1/m_1^a and stiffness ratio s_1/s_1^a are 0.58, 6.45 and 21.10, respectively. And dissipative mechanism is not considered in order to exactly find the coupled natural frequencies: $R_i = 0$.

In each case study, the non-dimensional natural frequencies Ω_i^c of the coupled systems are calculated for the change in the mass ratio, the stiffness ratio, a neck's position and cross-sectional area ratio. Mass ratio and stiffness ratio are multiplied by 1/4, 1/2, 1, 2 and 4 with the equivalent mass and stiffness of the acoustic medium constant. A neck has three positions: center, edge and a mid-point between two positions. And, the cross-sectional area ratio has five values: one-tenth; two-tenth; three-tenth; four-tenth; and five-tenth. Also, the theoretical resonance frequencies are calculated by MATLAB and results in Case study I-a are compared with those obtained from finite element analysis (SYSNOISE 5.5) for validating accuracy with regard to simplifications.

3.1. Case study I: double cavities blocked by an oscillator at one end

Double cavities investigated in this case study are connected by a neck and blocked by an oscillator at $x = b$ as shown in Fig. 2. The acoustic impedance at $x = 0^+$ becomes infinite ($\bar{Z}_{0^+} \to \infty$) and the characteristic

equation, which is deduced from Eqs. (15)–(20), can be represented by Eq. (23).

$$\Omega\pi\frac{m_1}{m_1^a}-\frac{1}{\Omega\pi}\frac{s_1}{s_1^a}-\frac{1/S_{21}\cot(\Omega\pi L_{21})-\Omega\pi L'_{n1}/S_{n1}-\tan(\Omega\pi)}{1+[1/S_{21}\cot(\Omega\pi L_{21})-\Omega\pi L'_{n1}/S_{n1}]\tan(\Omega\pi)}=0. \tag{23}$$

This equation shows that the natural frequencies of the coupled system depend on the non-dimensional effective length L'_{n1} depending on the neck's position and the cross-sectional area ratio S_{n1} as well as the mass ratio m_1/m_1^a and the stiffness ratio s_1/s_1^a. S_{21} and L_{21} could affect natural frequencies, but their effect will not be investigated in this work because width and length of a car with a trunk are very difficult to change in order to tune the acoustic natural frequency after the design process from a practical point of view.

3.1.1. Case study I-a: double cavities blocked by the first oscillator at one end ($\Omega^s<\Omega_1^a$)

Tables 1–4 show that the resonance frequencies calculated by our proposed method are very close to those obtained from FEA (SYSNOISE 5.5) within a tolerance of 2.11 percent. Fig. 3 shows the first four non-dimensional natural frequencies of the coupled system with four factors. Fig. 3(a) and (b) show the effects of mass and stiffness on the coupled system, respectively. Only the first natural frequency Ω_1^c, which represents the structural-controlled mode, increases with decreasing mass ratio and with stiffness ratio, but the other frequencies, which represent cavity-controlled modes, hardly changes. And it is interesting to compare the difference between the first two natural frequencies for the stiffness ratio multiplied by 4 and those for the mass ratio multiplied by 1/4. The proximity of uncoupled natural frequencies is the same, but the degree of coupling, the difference of two put-away frequencies, is greater in the latter than that in the former. Figs. 3(c) and (d) represent the effect of a neck on the coupled system. While the natural frequencies of the structural-controlled modes remain constant for the neck's position and cross-sectional area, those of the cavity-controlled modes decrease as the neck approaches the corner from the center but increase with the cross-sectional area.

3.1.2. Case study I-b: double cavities blocked by the second oscillator at one end ($\Omega^s=\Omega_1^a$)

Figs. 4(a) and (b) show the variation of the natural frequency with mass ratio and stiffness ratio of the coupled system for $\Omega^s=\Omega_1^a$. Although two new natural frequencies are split around the uncoupled natural

Table 1
Comparison of non-dimensional resonance frequencies by theory and FEA: stiffness effect (Case study I-a)

s_1/s_1^a ($\times 2.77$)	1/4	1/2	1	2	4
Ω_1^c					
Theory	0.145	0.176	0.226	0.301	0.408
FEA	0.142	0.174	0.224	0.300	0.408
Difference (%)	2.11	1.15	0.89	0.33	0.00
Ω_2^c					
Theory	0.587	0.587	0.588	0.590	0.596
FEA	0.592	0.592	0.593	0.595	0.601
Difference (%)	0.84	0.84	0.84	0.84	0.83
Ω_3^c					
Theory	1.159	1.159	1.159	1.159	1.160
FEA	1.160	1.160	1.160	1.161	1.161
Difference (%)	0.09	0.09	0.09	0.17	0.09
Ω_4^c					
Theory	2.068	2.068	2.068	2.068	2.069
FEA	2.062	2.062	2.062	2.062	2.063
Difference (%)	0.29	0.29	0.29	0.29	0.29

$$\text{Difference (\%)}=\left|\frac{\text{FEA}-\text{Theory}}{\text{FEA}}\right|\times 100.$$

Table 2
Comparison of non-dimensional resonance frequencies by theory and FEA: mass effect (Case study I-a)

m_1/m_1^a ($\times 6.45$)	1/4	1/2	1	2	4
Ω_1^c					
Theory	0.392	0.306	0.226	0.163	0.116
FEA	0.393	0.305	0.224	0.162	0.116
Difference (%)	0.25	0.33	0.89	0.62	0.00
Ω_2^c					
Theory	0.638	0.602	0.588	0.582	0.579
FEA	0.641	0.607	0.593	0.587	0.585
Difference (%)	0.47	0.82	0.84	0.85	1.03
Ω_3^c					
Theory	1.197	1.171	1.159	1.153	1.150
FEA	1.195	1.172	1.160	1.155	1.153
Difference (%)	0.17	0.09	0.09	0.17	0.26
Ω_4^c					
Theory	2.091	2.076	2.068	2.065	2.063
FEA	2.084	2.070	2.062	2.059	2.058
Difference (%)	0.33	0.29	0.29	0.29	0.24

$$\text{Difference (\%)} = \left|\frac{\text{FEA} - \text{Theory}}{\text{FEA}}\right| \times 100.$$

Table 3
Comparison of non-dimensional resonance frequencies by theory and FEA: effect of the neck's position (Case study I-a)

g_n/h_1	0	0.3	0.6	0.9
Ω_1^c				
Theory	0.226	0.226	0.226	0.225
FEA	0.224	0.224	0.224	0.224
Difference (%)	0.89	0.89	0.89	0.45
Ω_2^c				
Theory	0.588	0.582	0.556	0.490
FEA	0.593	0.585	0.560	0.495
Difference (%)	0.84	0.51	0.71	1.01
Ω_3^c				
Theory	1.159	1.152	1.130	1.093
FEA	1.160	1.151	1.127	1.088
Difference (%)	0.09	0.09	0.27	0.46
Ω_4^c				
Theory	2.068	2.059	2.044	2.032
FEA	2.062	2.049	2.033	2.022
Difference (%)	0.29	0.49	0.54	0.49

$$\text{Difference (\%)} = \left|\frac{\text{FEA} - \text{Theory}}{\text{FEA}}\right| \times 100.$$

frequency, only the natural frequency related to structural-controlled mode abruptly changes with the mass ratio or the stiffness ratio; but the other natural frequencies hardly change. But, the change in the neck's position and cross-sectional area affects not only the cavity-controlled modes but also the

Table 4
Comparison of non-dimensional resonance frequencies by theory and FEA: effect of the neck's cross-sectional area (Case study I-a)

h_n/h_1	0.1	0.2	0.3	0.4	0.5
Ω_1^c					
Theory	0.226	0.226	0.226	0.227	0.227
FEA	0.224	0.225	0.225	0.225	0.225
Difference (%)	0.89	0.44	0.44	0.89	0.89
Ω_2^c					
Theory	0.588	0.643	0.677	0.702	0.720
FEA	0.593	0.647	0.680	0.704	0.720
Difference (%)	0.84	0.93	0.44	0.28	0.00
Ω_3^c					
Theory	1.159	1.217	1.269	1.317	1.360
FEA	1.160	1.222	1.278	1.328	1.372
Difference (%)	0.09	0.41	0.70	0.82	0.58
Ω_4^c					
Theory	2.068	2.091	2.113	2.135	2.157
FEA	2.062	2.085	2.109	2.132	2.154
Difference (%)	0.29	0.29	0.19	0.15	0.14

$$\text{Difference (\%)} = \left|\frac{\text{FEA} - \text{Theory}}{\text{FEA}}\right| \times 100.$$

structural-controlled mode as shown in Figs. 4(c) and (d) although the degree of shift in natural frequency related to structural-controlled mode is small. All natural frequencies decrease with the distance g_n between the centers of the neck and the cavity and increase with the neck's cross-sectional area.

3.2. Case study II: double cavities blocked by two oscillators at both sides

As shown in Fig. 1, case study II considers double cavities blocked at both ends by two oscillators, whose physical and modal properties are equal to each other. Assuming that the external force to the mechanical oscillator at $x = 0^-$ does not exit, acoustic impedance $\bar{Z}_{0^-}$ at the point is zero. Therefore, $\bar{Z}_{0^+}$ and the characteristic equation, which is deduced from Eqs. (15)–(22), can be expressed by Eqs. (24) and (25), respectively.

$$\bar{Z}_{0^+} = -\bar{Z}_0^{(m)} = -\frac{Z_0^{(m)}}{S_2^2 Z_{c_1}} = -\frac{1}{S_{21}}\left(\frac{R_2}{\rho c S_2} + \mathrm{j}\left(\Omega\pi\frac{m_2}{m_2^a}L_{21} - \frac{1}{\Omega\pi}\frac{s_2}{s_2^a}\frac{1}{L_{21}}\right)\right), \tag{24}$$

$$\mathrm{Im}[\bar{Z}_b^{(m)}] + \frac{\dfrac{1}{S_{21}}\dfrac{\mathrm{Im}[\bar{Z}_0^{(m)}]S_{21} + \tan(\Omega\pi L_{21})}{1 - \mathrm{Im}[\bar{Z}_0^{(m)}]S_{21}\tan(\Omega\pi L_{21})} + \Omega\pi L'_{n1}/S_{n1} + \tan(\Omega\pi)}{1 - \left[\dfrac{1}{S_{21}}\dfrac{\mathrm{Im}[\bar{Z}_0^{(m)}]S_{21} + \tan(\Omega\pi L_{21})}{1 - \mathrm{Im}[\bar{Z}_0^{(m)}]S_{21}\tan(\Omega\pi L_{21})} + \Omega\pi L'_{n1}/S_{n1}\right]\tan(\Omega\pi)} = 0. \tag{25}$$

3.2.1. Case study II-a: double cavities blocked by the first oscillator at both ends ($\Omega^s < \Omega_1^a$)

Fig. 5 shows the first five natural frequencies changing with the four factors. The first two natural frequencies Ω_1^c and Ω_2^c, which represent the structural-controlled modes in each figure, are split around the non-dimensional natural frequency $\Omega^s$of the oscillator. They are strongly affected by the stiffness ratio, but cavity-controlled modes are not as shown in Fig. 5(a). And the difference $|\Omega_1^c - \Omega_2^c|$ between two split natural frequencies increases as the mass ratio decreases, and the non-dimensional natural frequency Ω_3^c of the

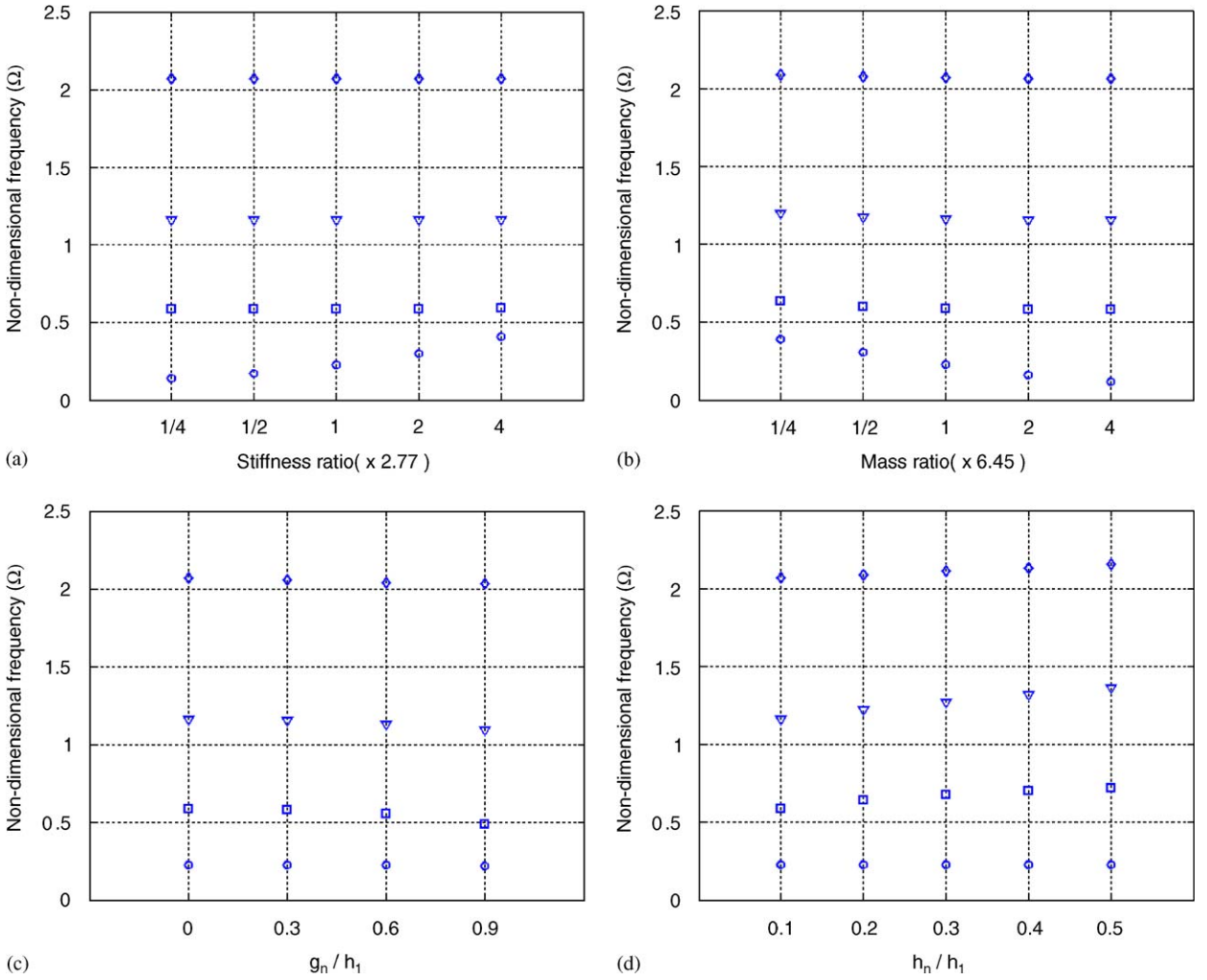

Fig. 3. Influence of four factors on natural frequency Ω_i^c for $\Omega^s < \Omega_1^a$ (Case study I-a): original stiffness ratio $(s_1/s_1^a) = 2.77$, original mass ratio $(m_1/m_1^a) = 6.45$, $\Omega_b^s = 0.21$ and $\Omega_1^a = 0.58$. (○) 1st natural frequency (Ω_1^c), (□) 2nd natural frequency (Ω_2^c), (▽) 3rd natural frequency (Ω_3^c) and (◇) 4th natural frequency (Ω_4^c). (a) Stiffness effect, (b) mass effect, (c) effect of the neck's position and (d) effect of the neck's cross-sectional area.

lowest-order cavity-controlled mode increases with decreasing mass ratio, as shown in Fig. 5(b). These results prove that the coupling degree of the coupled system depends on not only the closeness of uncoupled natural frequencies but also the mass ratio. That is, it increases as the density of acoustic medium increases or mass of structure system decreases. Figs. 5(c) and (d) display the natural frequencies, which change with the neck's position and cross-sectional area and show behavior similar to the results obtained in case study I-a. The non-dimensional natural frequencies of the cavity-controlled modes decrease as the neck approaches the corner from the center, and they increase with the cross-sectional area of the neck.

3.2.2. *Case study II-b: double cavities blocked by the second oscillator at both ends* ($\Omega^s = \Omega_1^a$)

In Fig. 6, the effect of the four factors on Ω_i^c of the coupled system is shown for $\Omega^s = \Omega_1^a$. The first two natural frequencies (Ω_1^c and Ω_2^c) of the coupled system represent structural-controlled modes, but they have the different relative motion of the oscillators. While two oscillators move in-phase at Ω_1^c, they move out-of-phase at Ω_2^c. Figs. 6(a) and (b) show that the change in the stiffness ratio and the mass ratio strongly affects the

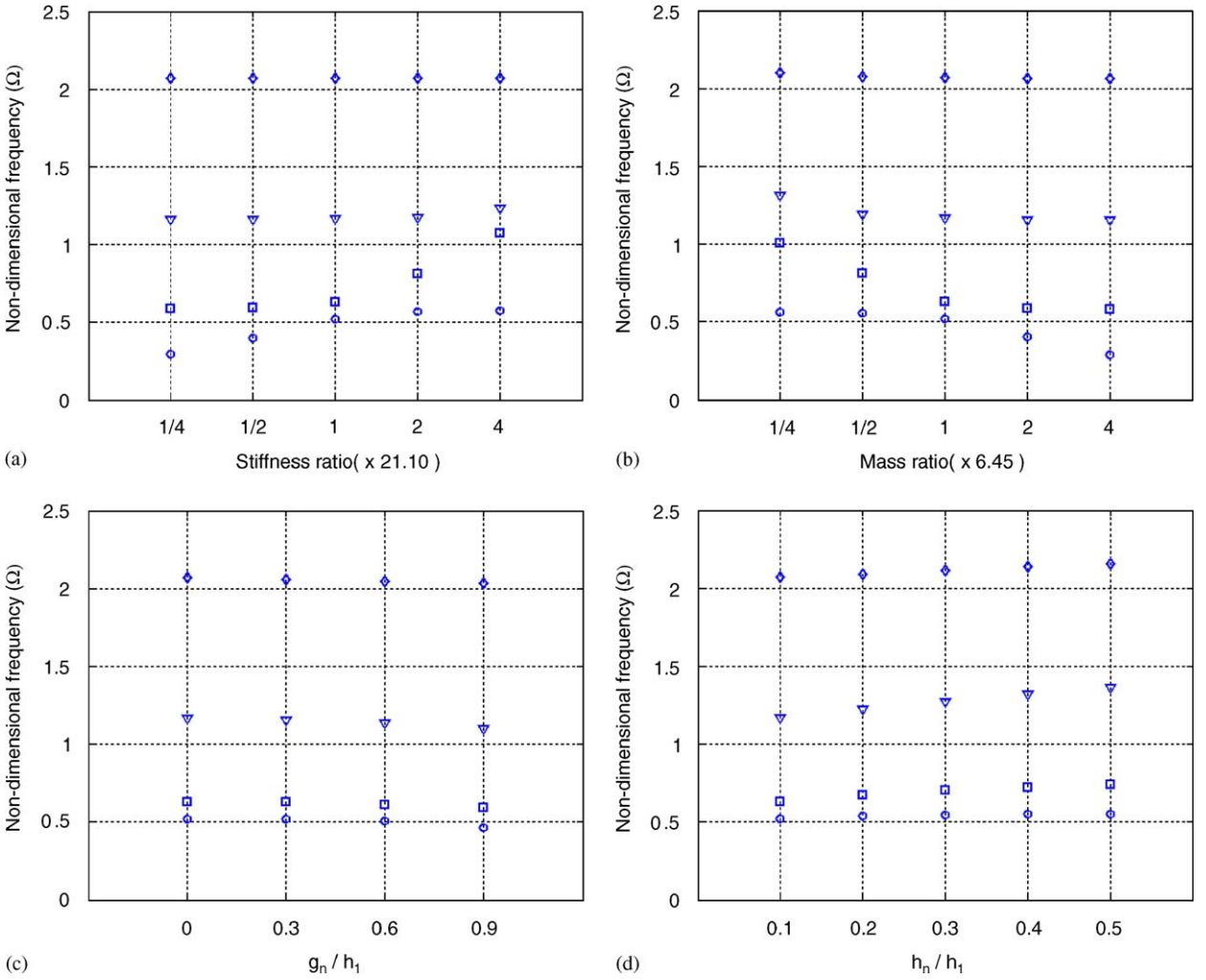

Fig. 4. Influence of four factors on natural frequency Ω_i^c for $\Omega^s = \Omega_1^a$ (Case study I-b): original stiffness ratio $(s_1/s_1^a) = 21.10$, original mass ratio $(m_1/m_1^a) = 6.45$ and $\Omega_1^a = \Omega_b^s = 0.58$. (○) 1st natural frequency (Ω_1^c), (□) 2nd natural frequency (Ω_2^c), (▽) 3rd natural frequency (Ω_3^c) and (◇) 4th natural frequency (Ω_4^c). (a) Stiffness effect, (b) mass effect, (c) effect of the neck's position and (d) effect of the neck's cross-sectional area.

structural-controlled modes, but hardly the cavity-controlled modes. Also they represent the increase in the difference of the two split natural frequencies with decrease in the mass ratio.

As the neck approaches the corner from the center, natural frequencies Ω_3^c, Ω_4^c and Ω_5^c of cavity-controlled modes decrease and natural frequency Ω_1^c of structural-controlled mode, which has two mechanical oscillators moving in-phase at both ends at Ω_1^c, also decreases in Fig. 6(c). This response is due to increase of the effective length of the neck with g_n/h_1. Fig. 6(d) shows that four natural frequencies (Ω_1^c, Ω_3^c, Ω_4^c and Ω_5^c) except for the 2nd natural frequency increase with the cross-sectional area of the neck. However, the second non-dimensional natural frequency Ω_2^c does not change because two oscillators move out-of-phase at Ω_2^c.

In summary, the natural frequencies of the coupled system depend on the mass ratio and the stiffness ratio between the structural system and the acoustic system, the neck's position and cross-sectional area, and the closeness of the natural frequencies of the uncoupled modes. The mass ratio and the stiffness ratio strongly affect the structural-controlled mode rather than the cavity-controlled modes. On the contrary, the cavity-controlled modes are affected strongly by the neck's position and cross-sectional area rather than the mass

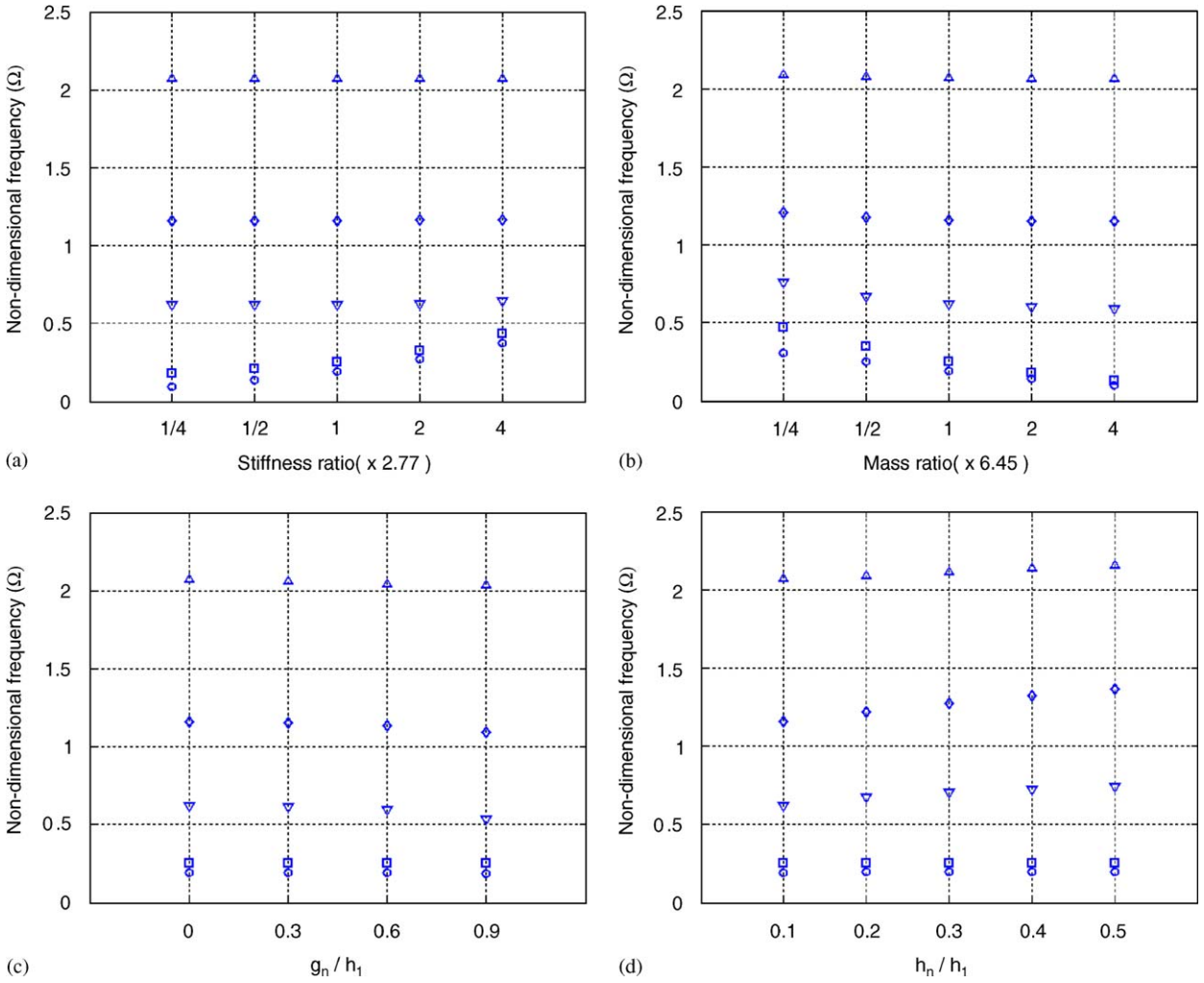

Fig. 5. Influence of four factors on natural frequency Ω_i^c for $\Omega^s < \Omega_1^a$ (Case study II-a): stiffness ratio = 2.77; mass ratio = 6.45; $\Omega_b^s = \Omega_0^s = 0.21$; and $\Omega_1^a = 0.58$. (○) 1st natural frequency (Ω_1^c), (□) 2nd natural frequency (Ω_2^c), (▽) 3rd natural frequency (Ω_3^c), (◇) 4th natural frequency (Ω_4^c) and (△) 5th natural frequency (Ω_5^c). (a) Stiffness effect, (b) mass effect, (c) effect of the neck's position and (d) effect of the neck's cross-sectional area.

ratio and the stiffness ratio. And the degree of coupling is affected by the closeness of the natural frequencies of uncoupled modes as well as the major four factors.

4. Discussions

Acoustic pressure distribution at each coupled mode and the relation between a new coupling parameter and natural frequencies are discussed by the use of the results obtained in case study II-b. The discussion centers on the effect of the neck's position and cross-sectional area on the modal properties of the coupled system. Also, the characteristics of the structure-controlled mode in our proposed theoretical model are briefly mentioned in terms of existence and non-existence of a trunk lid and in terms of the coupling degree.

Fig. 7 shows the first five acoustic modes of the coupled system used in Case study II-b (Refer to [29]). In all coupled modes, the acoustic pressure distribution around the neck is strongly affected by the evanescent wave, but that of the point away from the neck is determined by the standing wave. Acoustic pressure near both ends

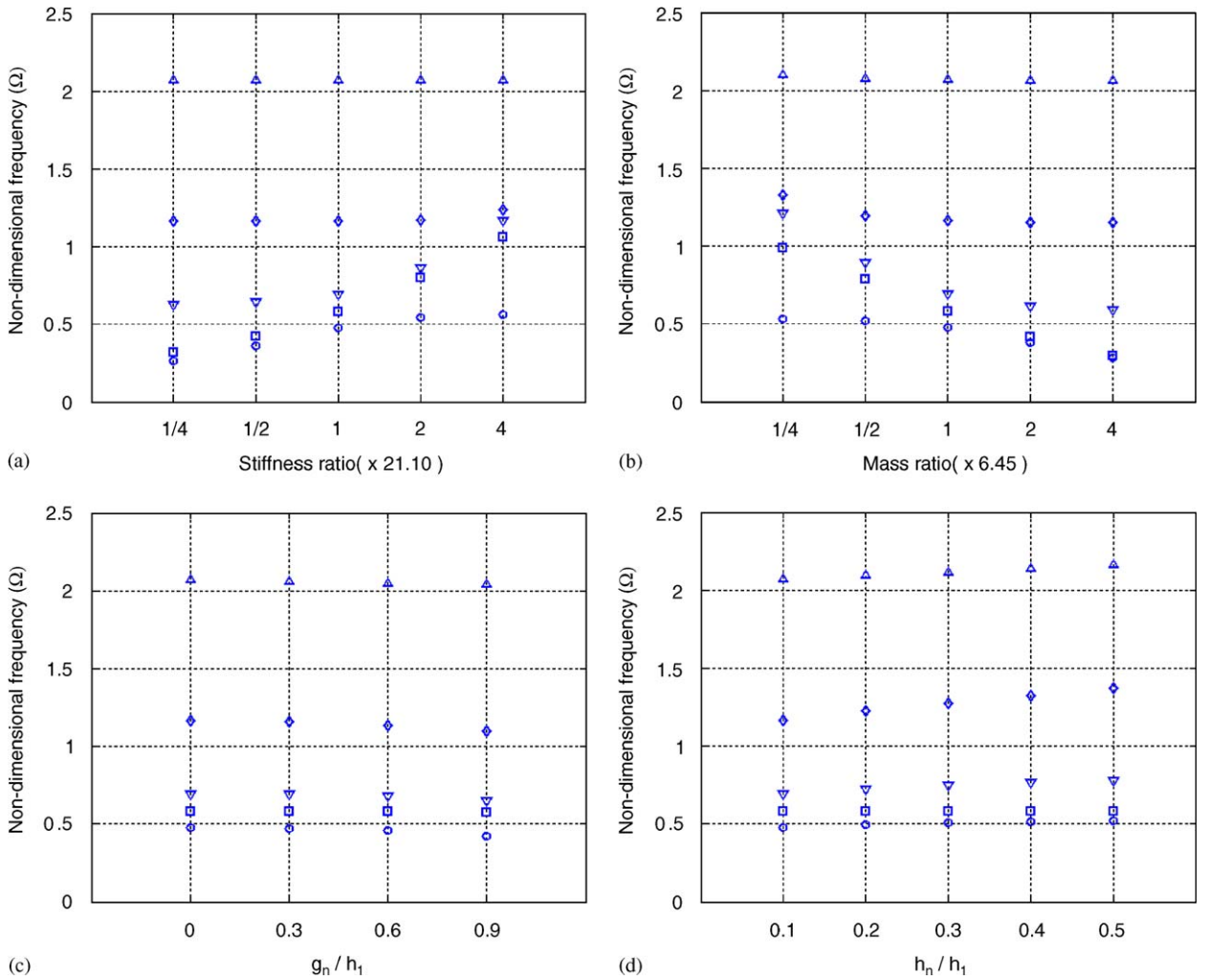

Fig. 6. Influence of four factors on natural frequency Ω_i^c for $\Omega^s = \Omega_1^a$ (Case study II-b): original stiffness ratio $(s_1/s_1^a) = 21.10$, original mass ratio $(m_1/m_1^a) = 6.45$, and $\Omega_b^s = \Omega_0^s = \Omega_1^a = 0.58$. (○) 1st natural frequency (Ω_1^c), (□) 2nd natural frequency (Ω_2^c), (▽) 3rd natural frequency (Ω_3^c), (◇) 4th natural frequency (Ω_4^c) and (△) 5th natural frequency (Ω_5^c). (a) Stiffness effect, (b) mass effect, (c) effect of the neck's position and (d) effect of the neck's cross-sectional area.

depends on the interaction between the acoustic medium and the mechanical oscillator. The first two coupled modes are structure-controlled modes, but the phases of the two oscillators at each mode are different from each other. The first mode at Ω_1^c has the same phase motion of the two oscillators at both ends, but two oscillators in the second mode at Ω_2^c have phase difference of 180 degree. Therefore, the first coupled mode has acoustic pressure distribution similar to that of a rigid-wall acoustic mode, and change in the associated natural frequency has the similar trend of the natural frequency of cavity-controlled mode changing with the neck's position and cross-sectional area. Acoustic pressure distribution in cavity-controlled modes is very similar to that in uncoupled cavity modes.

The natural frequencies of our proposed theoretical model are inversely proportional to the new acoustic parameter. Fig. 8 shows the effect of the neck's position on the natural frequency of coupled modes. As g_n/h_1 increases, the associated natural frequency decreases and the value of the new coupling parameter L'_{n1}/S_{n1} increases. It is because rise in the number of cross-modes, which are generated due to existence of the neck, increases added length as the neck approaches the edge from the center [29]. When the cross-sectional area ratio is constant ($S_{n1} = 0.1$), the increase in the effective length decreases the natural frequency of the

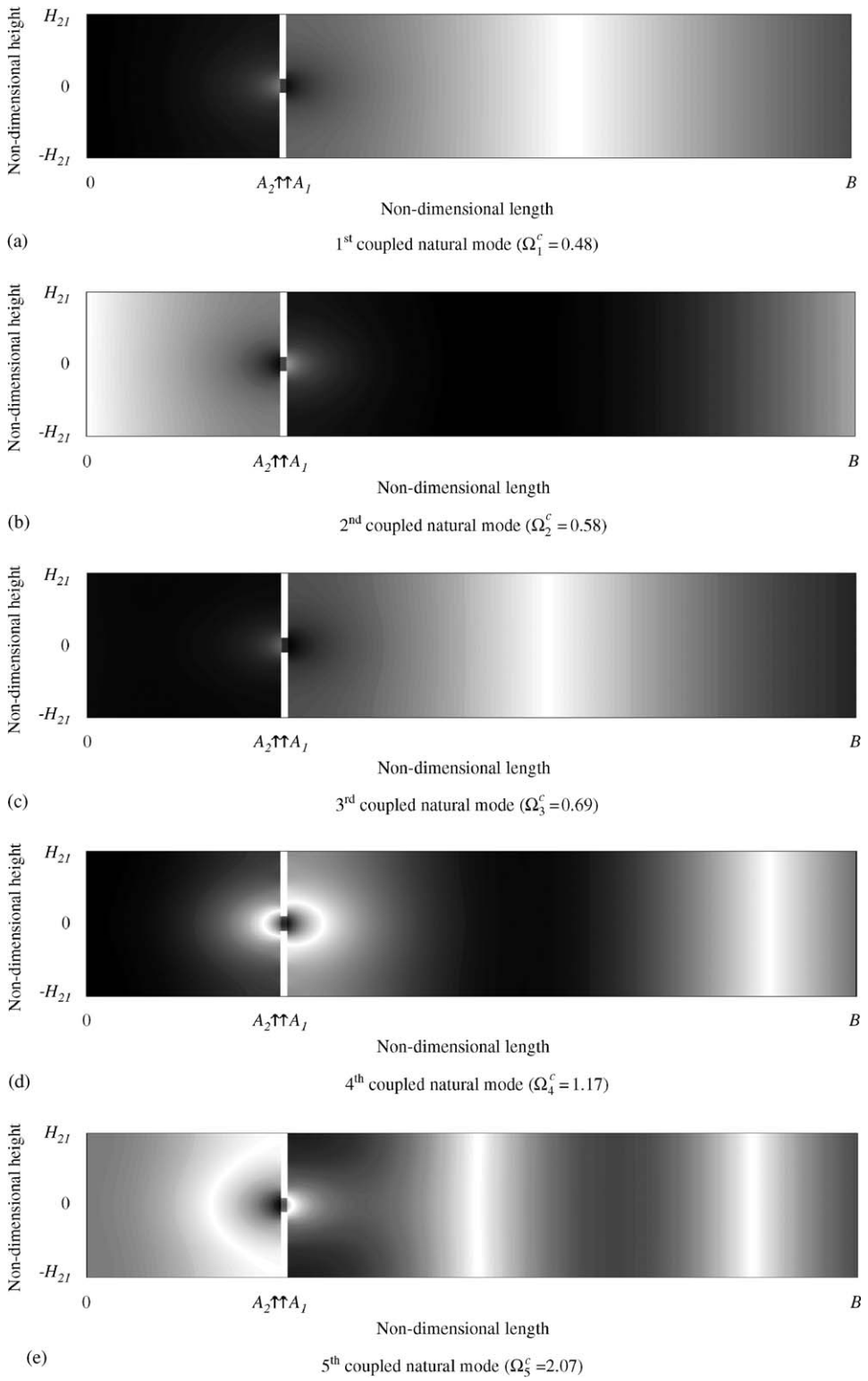

Fig. 7. Natural modes of the coupled system for $\Omega^s = \Omega_1^a$ (Case study II-b). A_1, A_2, B are non-dimensional points (a_1/l_1, a_2/l_1, b/l_1). Absolute value of acoustic pressure: 

. (a) 1st coupled natural mode ($\Omega_1^c = 0.48$), (b) 2nd coupled natural mode ($\Omega_2^c = 0.58$), (c) 3rd coupled natural mode ($\Omega_3^c = 0.69$), (d) 4th coupled natural mode ($\Omega_4^c = 1.17$) and (e) 5th coupled natural mode ($\Omega_5^c = 2.07$).

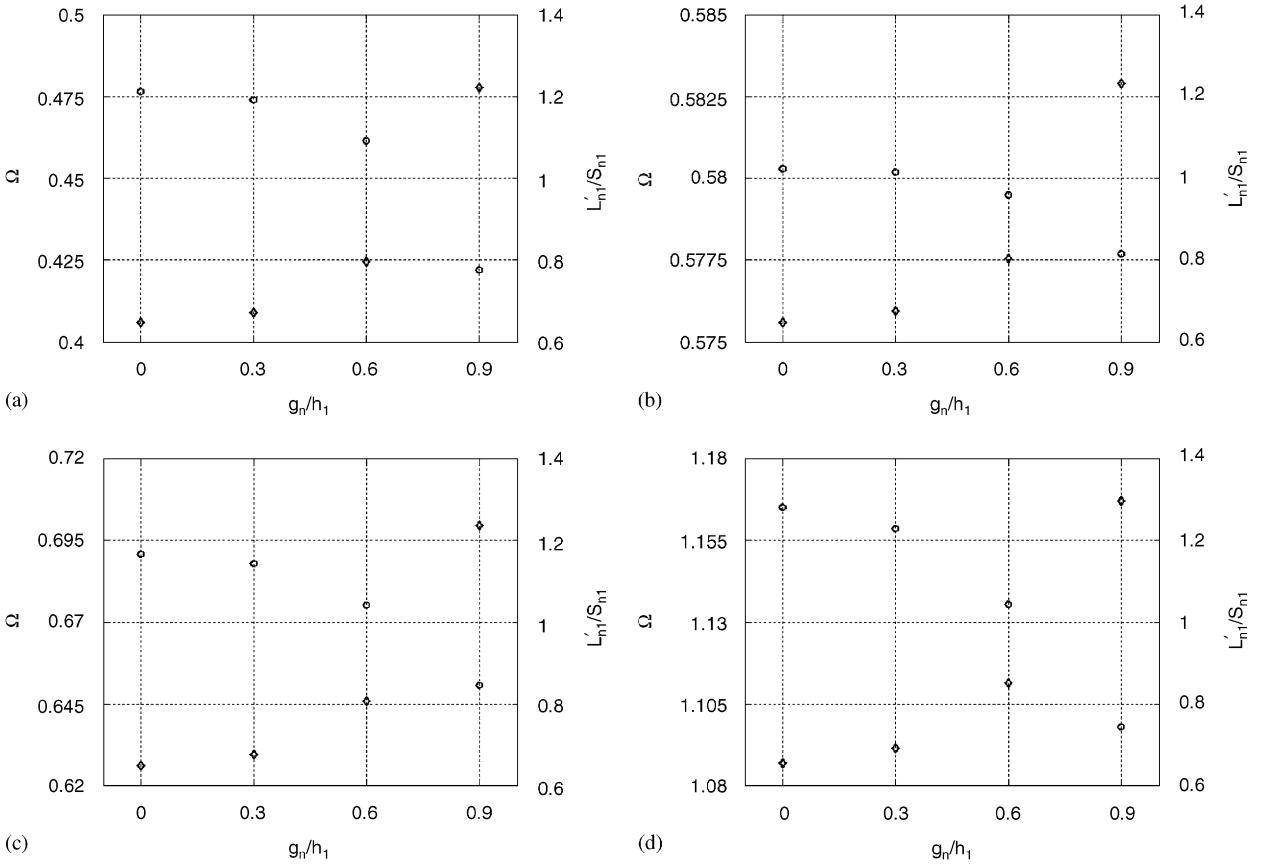

Fig. 8. Relationship between the non-dimensional natural frequency and the new coupling parameter with the neck's position for $\Omega^s = \Omega_1^a$ (Case study II-b): (○) natural frequency (Ω_i^c) and (◇) a new coupling parameter (L'_{n1}/S_{n1}). (a) 1st natural frequency, (b) 2nd natural frequency, (c) 3rd natural frequency and (d) 4th natural frequency.

associated coupled mode. Fig. 9 shows the effect of the neck's cross-sectional area on the natural frequencies of the coupled system in terms of the change in the new coupling parameter L'_{n1}/S_{n1}. All natural frequencies decrease with the increase in the value of the new coupling parameter. The decreasing rate of the structure-controlled mode (the 1st mode) is much less than that of the cavity-controlled mode (the 3rd and 4th mode). But, the decreasing rate of the structure-controlled mode is comparable to that of the cavity-controlled mode.

A theoretical model including a trunk lid may have another structural-controlled mode, but the existence of a trunk lid does not strongly affect the degree of coupling. The closeness of uncoupled natural frequencies is more important to the coupled system than the existence and non-existence of the trunk lid. Also, only structural-controlled modes whose acoustic pressure distribution is similar to that of rigid-wall acoustic modes or cavity-controlled modes are strongly affected by the change in a neck's characteristics.

5. Conclusions

This paper suggested a new theoretical model to investigate interior noise in a passenger compartment with a trunk compartment. The new model was a coupled structural–acoustic system composed of double cavities connected by a neck and mechanical oscillators as shown in Fig. 1. In order to obtain the characteristic equation, forced vibro-acoustical analysis was applied to the coupled system, and the plane wave theory was used. Input acoustic impedance was written by the series summation of acoustic impedances calculated at the surface of discontinuity in the cross-sectional area. Especially, evanescent waves as well as standing waves were considered to investigate the effect of neck's position and cross-sectional area on the natural frequencies

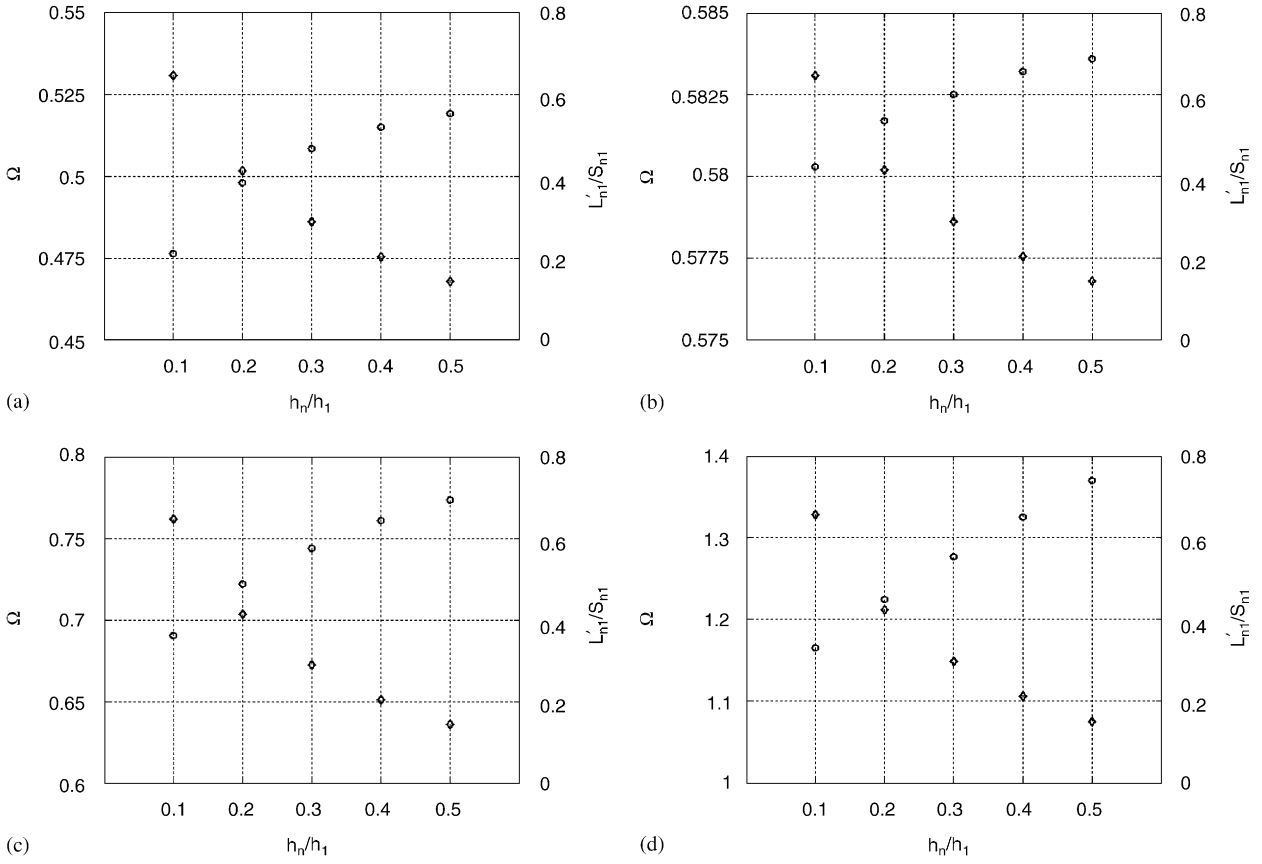

Fig. 9. Relationship between the non-dimensional natural frequency and the new coupling parameter with a cross-sectional area of a neck for $\Omega^s = \Omega_1^a$ (Case study II-b): (○) Natural frequency (Ω_i^c) and (◇) a new coupling parameter (L'_{n1}/S_{n1}). (a) 1st natural frequency, (b) 2nd natural frequency, (c) 3rd natural frequency and (d) 4th natural frequency.

of a coupled system. A new coupling parameter was derived to explain the dynamic behavior of a coupled structural–acoustic system including double cavities connected by a neck.

Longitudinal mode, which is strongly related to the booming noise of an automobile with a trunk, was examined in terms of mass ratio, stiffness ratio, a neck's position and cross-sectional area. While the effect of structural modification (change in mass ratio and stiffness ratio) is limited to structural-controlled modes, the change in a neck's characteristics, which are represented by a new parameter L'_{n1}/S_{n1} (non-dimensional effective length of a neck divided by a cross-sectional area ratio), affects not only cavity-controlled modes but also structural-controlled modes whose acoustic pressure distribution is similar to that of rigid-wall acoustic modes or cavity-controlled modes. The natural frequencies are inversely proportional to the new coupling parameter. They increase as a neck approaches the center from the corner and a neck's cross-sectional area increases.

In conclusions, the acoustic modal properties of a passenger compartment of an automobile with a trunk can be modified by changing the position and cross-sectional area of the necks on the package tray, which partitions the passenger compartment from the trunk. The effect of a neck's cross-sectional area and position will be qualitatively investigated in the experiments of the companion paper, Part 2.

Acknowledgment

This work was supported by the Brain Korea 21 Project in 2005.

References

[1] S.H. Kim, J.M. Lee, Practical method for noise reduction in a vehicle passenger compartment, *Journal of Vibration and Acoustics* 120 (1998) 199–205.

[2] C.J. Chapman, S.V. Sorokin, The forced vibration of an elastic plate under significant fluid loading, *Journal of Sound and Vibration* 284 (2005) 1131–1144.

[3] J. Pan, D.A. Bies, The effect of fluid–structural coupling on sound waves in an enclosure—theoretical part, *Journal of the Acoustical Society of America* 87 (2) (1990) 691–707.

[4] J. Pan, D.A. Bies, The effect of fluid–structural coupling on sound waves in an enclosure—experimental part, *Journal of the Acoustical Society of America* 87 (2) (1990) 708–717.

[5] K.L. Hong, J. Kim, Analysis of free vibration of structural–acoustic coupled systems, part II: two- and three-dimensional examples, *Journal of Sound and Vibration* 188 (4) (1995) 577–600.

[6] J.M. Mondot, B. Petersson, Characterization of structure-borne sound sources: the source descriptor and the coupling function, *Journal of Sound and Vibration* 114 (3) (1987) 507–518.

[7] Z. Ma, I. Hagiwara, Improved mode-superposition technique for modal frequency response analysis of coupled acoustic–structural systems, *AIAA* 29 (10) (1991) 1720–1726.

[8] J.A. Wolf Jr., Modal synthesis for combined structural–acoustic systems, *AIAA* 15 (1977) 734–745.

[9] S. Van Lier, The vibro-acoustic modeling of slab track with embedded rails, *Journal of Sound and Vibration* 231 (3) (2000) 805–817.

[10] S.W. Kang, J.M. Lee, S.H. Kim, Structural–acoustic coupling analysis of the vehicle passenger compartment with the roof, air-gap, and trim boundary, *Journal of Vibration and Acoustics: ASME* 122 (2000) 196–202.

[11] T. Osawa, A. Iwama, A study of the vehicle acoustic control for booming noise utilizing the vibration characteristics of trunk's lid, *SAE* 861410 (1986).

[12] F. Cura, G. Curti, M. Mantovani, Study of the forced response of a clamped circular plate coupled to a uni-dimensional acoustic cavity, *Journal of Sound and Vibration* 190 (4) (1996) 661–675.

[13] F. Scarpa, G. Curti, A method for the parametric frequency sensitivity of interior acoustic–structural coupled systems, *Applied Acoustics* 58 (1999) 451–467.

[14] K.L. Hong, J. Kim, Analysis of free vibration of structural–acoustic coupled systems, Part I: development and verification of the procedure, *Journal of Sound and Vibration* 188 (4) (1995) 561–572.

[15] K.L. Hong, J. Kim, New analysis method for general acoustic–structural coupled systems, *Journal of Sound and Vibration* 192 (2) (1996) 465–480.

[16] R.H. Lyon, Noise reduction of rectangular enclosures with one flexible wall, *Journal of the Acoustical Society of America* 35 (11) (1963) 1791–1797.

[17] M.D.C. Magalhaes, N.S. Ferguson, Acoustic–structural interaction analysis using the component mode synthesis method, *Applied Acoustics* 64 (2003) 1049–1067.

[18] E.H. Dowell, H.M. Voss, The effect of a cavity on panel vibration, *AIAA* 1 (1962) 476–477.

[19] S.H. Sung, D.J. Nefske, A coupled structural–acoustic finite element model for vehicle interior noise analysis, *Journal of Vibration, Acoustics, Stress, and Reliability in Design: ASME* 106 (1984) 314–318.

[20] D.J. Nefske, J.A. Wolf Jr., L.J. Howell, Structural–acoustic finite element analysis of the automobile passenger compartment: a review of current practice, *Journal of Sound and Vibration* 80 (2) (1982) 247–266.

[21] F. Han, L.G. Mongeau, R.J. Bernard, A model for the vibro-acoustic response of plates excited by complex flows, *Journal of Sound and Vibration* 246 (5) (2001) 901–926.

[22] N. Trompette, M. Guerich, An experimental validation of vibro-acoustic prediction by the use of simplified methods, *Applied Acoustics* 66 (2005) 427–445.

[23] B. Campbell, M. Abrishaman, W. Stokes, Structural–acoustic analysis for the prediction of vehicle body acoustic sensitivities, *SAE* 931327 (1993) 507–516.

[24] D.D. Reynolds, *Engineering Principles of Acoustics-nose and Vibration Control*, Allyn and Bacon, Inc., Boston, 1981.

[25] R.C. Chanaud, Effects of geometry on the resonance frequency of Helmholtz resonators, part II, *Journal of Sound and Vibration* 204 (5) (1997) 829–834.

[26] J.W. Miles, The analysis of plane discontinuities in cylindrical tubes. Part I, *Journal of the Acoustical Society of America* 17 (3) (1946) 259–271.

[27] L. Cremer, M. Heckl, *Structure-borne Sound: Structure Vibrations and Sound Radiation at Audio Frequencies*, Springer, New York, 1972.

[28] L.E. Kinsler, A.R. Frey, A.B. Coppens, J.V. Sanders, *Fundamentals of Acoustics*, Wiley, New York, 1982.

[29] J.W. Lee, J.M. Lee, S.H. Kim, Acoustical analysis of multiple cavities connected by necks in series with a consideration of evanescent waves, *Journal of Sound and Vibration* 273 (2004) 515–542.